physics

MDPI

Article

Hunting for Dwarf Galaxies Hosting the Formation and Coalescence of Compact Binaries

Luca Graziani [1,2,3,†]

[1] Dipartimento di Fisica, Sapienza, Università di Roma, Piazzale Aldo Moro 5, 00185 Roma, Italy; luca.graziani@uniroma1.it
[2] INFN, Sezione di Roma I, P.le Aldo Moro 2, 00185 Roma, Italy
[3] INAF/Osservatorio Astrofisico di Arcetri, Largo E. Femi 5, 50125 Firenze, Italy
† Current address: Dipartimento di Fisica, Sapienza, Università di Roma, Piazzale Aldo Moro 5, 00185 Roma, Italy.

Received: 4 November 2019; Accepted: 3 December 2019; Published: 6 December 2019

Abstract: Here we introduce the latest version of the GAMESH model, capable to consistently account for the formation and evolution of compact binary systems along the cosmic assembly of a Milky Way (MW)-like galaxy, centered on a local group volume resolving a large population of dwarf satellites. After describing the galaxy assembly process and how the formation of binary systems is accounted for, we summarize some recent findings on the properties and evolution of low-metallicity dwarf galaxies hosting the birth/coalescence of stellar/compact binaries generating GW150914-like signals. Finally, we focus on the mass and orbital properties of the above compact binary candidates assessing their impact on the resulting coalescence times and on selecting suitable galaxy hosts.

Keywords: galaxy formation; galaxy evolution; dwarf galaxies; compact binary systems; multi-messenger astronomy

1. Introduction

The detection of three gravitational wave (GW) signals GW150914, GW151226, and GW151012 during the first advanced Laser Interferometer Gravitational-Wave Observatory (LIGO) observing run "O1", performed from 12 September 2015 to 19 January 2016 [1–5], marked the birth of gravitational astronomy. The successive observing run "O2", by the joint advanced LIGO–VIRGO detectors (30 November 2016–25 August 2017), provided seven additional GW signals interpreted as black hole binary (BHBH) mergers and one GW signal likely originated from the coalescence of binary neutron stars (NSNS) [5]. So far, the ongoing run "O3" [6] has generated intriguing event alerts (https://gracedb.ligo.org/latest/) with a remarkably high luminosity distance.

Once confirmed as GW detection, the integrated catalogue of all the above events promises to provide a robust observational data set on which both theoretical and phenomenological models of BHBH formation and evolution can rely as an independent source of physical constraints [7]. Many alternative approaches have been developed during the recent years, either based on population synthesis methods [8–14] or on schemes of dynamical capture acting in stellar clusters [15–19] and in galactic nuclei [20]. Both the formation mechanism and the galactic environment have a strong impact on the physical properties of the formed binaries, such as masses, spin, and orbital parameters. A recent study [21] suggested for example, that the most massive BHBH could be part of a primordial population formed in the early Universe.

The same observations apply, on a cosmological context, to galaxy evolution models [22–25] because the simultaneous detection of gravitational and electromagnetic signals could significantly constrain both the predicted cosmic star formation history and the galaxy properties, along the redshift

evolution of our universe. Although BHBH events are not expected to have an electromagnetic counterpart [26] (but see Perna et al. [27] for an alternative theoretical scenario), the discovery of a NSNS merger in "O2" opens the possibility of a synergy between gravitational detectors and traditional telescopes operating in different bands of the electromagnetic spectrum [28,29]. Present theoretical models need substantial improvements in order to get ready for multi-messenger astrophysics, as they have to self-consistently predict both GW events and their electromagnetic counterparts [30] along the galaxy formation process.

Since the detection of GW150914, several groups focused on computing the rates of different merging systems (either BHBH or NSNS) and on describing the type of galaxies candidate to host these events. Dominik et al. [9] estimated the merger rates by coupling a binary synthesis population code with cosmological scaling relations available for the star formation history and metallicity. Nowadays, a complementary approach is offered by hydrodynamical simulations which provide a consistent description of the cosmic star formation in the context of the galaxy evolution. Mapelli et al. [31], for example, randomly sampled the galaxy catalogue of the Illustris Simulation [32] to predict the above rates and to identify the properties of the galaxies hosting coalescence events (see Artale et al. [33]). Lamberts et al. [34] adopted the feedback-rich, FIRE (Feedback In Realistic Environments) hydrodynamical simulation suite [35,36] to estimate the population of BHBH in the Milky Way (MW) simulated in the "Latte" run. Each approach has its own advantages and drawbacks: fast predictions and parameter explorations can be easily generated by combining semi-analytic star formation recipes with binary synthesis codes but at the price of avoiding any characterization of the galaxies hosting the signals. Both smooth particle hydrodynamics (SPH) and adaptive mesh refinement (AMR)-based simulations show additional limitations in the fact that they need to assume a minimum dark matter (DM) mass or a minimum spatial resolution when describing their cosmic structures, so that the validity of the results across scales often requires convergence verification. Finally, it is worth to mention that to reach the local universe epoch ($z = 0$) numerical simulations still require significant computational resources and can not easily fine tune the efficiency of the implemented feedback.

Recent hydrodynamical simulations [35,37,38] evolve their structures under a rich series of feedback effects, although they remain severely limited, with few exceptions [39,40], in describing the reionization process, responsible for the ionization and heating of the intergalactic medium (IGM). The process of cosmic reionization, which prevents the gas of the IGM to cool and collapse into galactic halos, plays a central role in regulating the efficiency of star formation in small objects, such as the population of dwarf galaxies [41]. Under photo-ionization feedback, dwarfs can remain trapped into inhomogeneously expanding HII regions and become unable to acquire fresh gas from the IGM because of their low DM halo potential (This is commonly expressed in terms of virial temperature $T_{\rm vir}$ of their halos).

To encompass some of these limitations and to provide an alternative tool addressing many of the above questions, in Graziani et al. [24] we introduced GAMESH, a hybrid pipeline which combines the outputs of a DM simulation, a semi-analytic model of star formation and metal enrichment with a detailed reionization model based on the latest versions of the state-of-art radiative transfer code CRASH [42,43]. While not necessarily limited to a small scale simulation, so far GAMESH has performed on top of local volume boxes (∼2–4 cMpc/side) to investigate the evolution of a Milky Way-like galaxy and its surrounding dwarf satellites. By easily tuning few efficiency parameters regulating the formation of stars and the mass of gas and metals ejected by galactic winds, we were capable to reproduce the metal, gas and stellar mass of the Milky Way-like halo at $z = 0$, as well as the scaling relations observed in the local group galaxies [25]. A first study of the local volume reionization and its impact on the galaxy metallicity function was presented in Graziani et al. [24], while the properties of the Milky Way progenitors and the dwarf satellites were reported in Graziani et al. [25]. GAMESH is continuously upgraded and improved both in the chemical and radiative modules: in Ginolfi et al. [44] for example, the chemical network of our galaxies

was extended by introducing the formation of cosmic dust by stellar sources. The latest release of the radiative transfer framework can consistently handle x-rays emitting sources and accounts for the physics of secondary ionization [43] through gas and dust [45]. In Schneider et al. [46], a major upgrade to the star formation model of GAMESH was introduced by characterizing the formation and evolution of binary systems. The statistic of compact binaries generating GW events through black hole mergers was first investigated, consistently with the metallicity of the gas in the galactic environment. The evolution of these binaries was also followed in redshift along the hierarchical assembly of structures, until their coalescence occurs at a certain z_c, in a certain galactic host, and accordingly to the binary system coalescing time t_c. This first analysis showed that signals like GW150914, GW151226 and GW151012-like are originated by coalescence events preferentially hosted in massive star forming galaxies, despite the fact that their binary systems were born in galaxies with different gas metallicity (see also independent studies by Lamberts et al. [47], Elbert et al. [48]). However, when we focus on the most massive BHBH systems (e.g., systems with BH masses $M_1 > 36\ M_\odot$ and $M_2 > 27\ M_\odot$), as their stellar progenitors can only form in low metallicity environments ($Z < 0.1\ Z_\odot$) [4,9,19,49], metal-poor dwarfs become the natural candidates to host the formation of these binaries. As dwarfs are not necessarily incorporated by massive galaxies during hierarchical evolution, isolated dwarfs, dwarf spheroidals, or ultra-faint satellites, can also become the galactic host of coalescence events. Motivated by the above findings, in Marassi et al. [50] we put our attention on describing the formation and evolution of low metallicity dwarf galaxies in which binaries generating GW150914-like events can be found. By following their histories throughout dynamical, chemical and radiative feedback, we connected birth and coalescence sites and provided a clue on their galactic evolution. We also indicated the most interesting evolutionary channels, highlighting how the gas metallicity of these objects can strongly vary due to continuous dynamical stripping, while orbiting around a central object (see Section 5 in Graziani et al. [25]). Sporadic episodes of star formation can also occur when they increase their gas mass against the effects of photo-ionization heating (see also Section 3 in Marassi et al. [50]). The above study was also reinforced by a serendipitous search of real observed counterparts: we found, for example, an excellent match between many properties of PGC1446233 [51] and UGC4483 [52] and two representative candidates of our simulated sample.

Here we first describe our GAMESH model and how it follows the evolution of compact systems along the assembly of its simulated galaxies. We then show its capabilities in accounting for different types of compact binaries and in predicting the galaxies hosting their formation and coalescence.

2. Numerical Method

This section summarizes the key ingredients of the GAMESH framework. We start with a galaxy formation model capable to resolve mini-halos and to follow the evolution of their embedded galaxies through a combination of feedback effects: dynamical, chemical, and radiative (see Section 2.1). The second ingredient is a binary population synthesis code which computes the formation and evolution of a large series of binary systems (see Section 2.2). Finally, the third component of our method couples the star formation history of each galaxy with a number of binary systems, randomly selected from our pre-computed database (see Section 2.3).

2.1. Galaxy Formation with GAMESH

The galaxy formation model described in this section was first introduced in Graziani et al. [24] and named GAMESH. The work-flow of GAMESH integrates a DM simulation based on a N-body scheme, a semi-analytic code modeling the galaxies created at the center of dark matter halos, and a radiative transfer module based on the cosmological RT library RT4C, on top of which the latest release of the radiative transfer code CRASH4 is built [43].

2.1.1. DM Halos

The DM simulation currently adopted by GAMESH predicts the cosmological evolution of a MW-sized halo and was performed with the GCD+ code [53,54] adopting a β-version of periodic-boundary conditions and a TreePM algorithm with parallel FFTW (Fastest Fourier Transform in the West) module. The code MUSIC [55], set up with a Planck 2013 cosmology [56] ($\Omega_0 = 0.32$, $\Lambda_0 = 0.78$, $\Omega_b = 0.049$ and $h = 0.67$), was used to generate an initial volume of 83.5^3 Mpc^3 in which a Milky Way-sized halo with virial mass of 1.7×10^{12} M$_\odot$ was first identified, and successively re-simulated with 62421192 DM particles of different masses; 55012200 of them have a particle mass of 3.4×10^5 M$_\odot$ and create a central volume with the highest mass resolution, a size of $L_b = 4$ cMpc and a total mass in collapsed objects of $\mathrm{M_{DM}} \sim 3 \times 10^{12}$ M$_\odot$. We usually refer the above 4 cMpc cosmic region as the "LG" of this simulation.

The temporal evolution is followed by storing outputs every 15 Myr from $z \sim 20$ down to $z = 10$, and every 100 Myr until $z = 0$. A total of 155 snapshots guarantees a time resolution capable to follow the primordial stellar systems and to accurately account for gas recombinations during reionization.

Each snapshot was post-processed by using a standard friend-of-friends (FoF) algorithm with a linking parameter of $b = 0.2$ and a minimum number of 100 particles to identify collapsed halos. For each object we also stored positions and velocities of all particles in order to study, when a sufficient number of particles is available, the halo internal structure (i.e., DM profiles, angular momentum, internal motion, over-density structures, etc.). At $z = 0$, the LG contains 2458 halos and more than 13,000 collapsed structures are found on a wider scale of 8 Mpc/side, while partially contaminated with particles at lower mass resolution. Two of the halos in the LG have a DM mass $\mathrm{M_{DM}} \sim 10^{11}$ M$_\odot$ and result similar to the ones estimated for M32, M33 or LMC-type in our local group (see Table 1 in Guo et al. [57] and references therein); 14 halos have $10^{10} \lesssim \mathrm{M_{DM}} < 10^{11}$ M$_\odot$, while 98 are found with $10^9 \lesssim \mathrm{M_{DM}} < 10^{10}$ M$_\odot$. It is important to note that this configuration is representative of an average MW-like halo found in large DM simulations and does not necessarily match the observed local volume because another massive object resembling to M31 is missing at the observed distance, while found within 8 cMpc (The absence of a M31-like halo within 4 cMpc implies that the total mass of the resolved volume is too low with respect to the observations because recent estimates suggests that $M_{\mathrm{M31}} \gtrsim M_{\mathrm{MW}}$ [58]).

For each halo we built its merger tree (MT) by searching its particles in all previous snapshots; when a certain particle is not associated with any halo, it becomes part of the diffuse intergalactic medium, as seen in DM (DIGM). In this way we can exactly follow all the dynamical interactions regulating the accretion of dark matter halos: mergers, tidal stripping, and halo disruptions. This approach is sufficiently flexible and accurate to implement a future particle tagging technique and to associate baryons and DM particles in order to mimic an inhomogeneous metal enrichment.

Finally, the spatial distribution of DM is obtained by mapping the particles on grids of $N_c = 512$ cells/side; this provides a spatial resolution of ~ 7.8 ckpc in mapping the LG. From these DM grids, the gas distribution is easily derived by scaling the DM mass with the value of the universal baryon fraction, constrained by our cosmology. Figure 1 shows a slice cut view of the LG volume at $z = 0$, in which the MW-like central galaxy and its satellites are still connected through a cosmic web of gas filaments. The same slice cut is shown in Figure 2a,b but refers to $z = 0.11$, i.e., the simulation image closest to the highest redshift value of the LIGO–VIRGO coalescence window for GW150914 ($z = 0.12$), as adopted in Marassi et al. [50]. The left panel (a) shows the LG volume while the right one (b) describes the cosmic web at the largest, 8 cMpc scale.

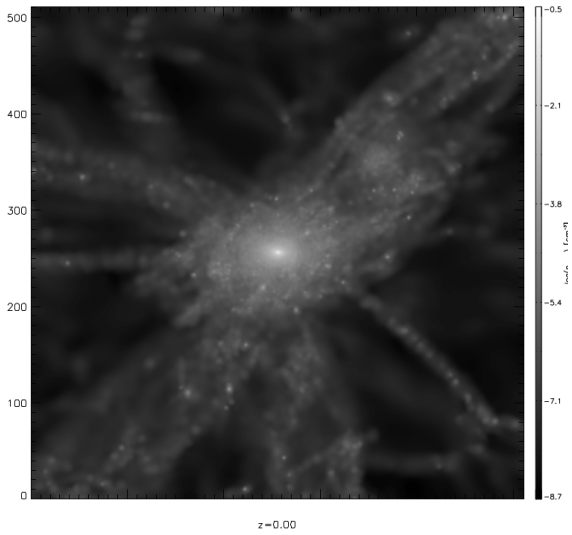

Figure 1. Slice cut at $z = 0$ of the LG volume (4^3 Mpc^3) in the GAMESH simulation described in Graziani et al. [25]. The cut intercepts the central MW-like galaxy and clearly shows a plethora of satellites orbiting the central object or falling into it along the filament of the surrounding cosmic web. The gray palette shows the logarithm of the gas number density (Log(n_{gas})), derived from the DM distribution and projected on a Cartesian grid of 512^3 cells (see text for more details).

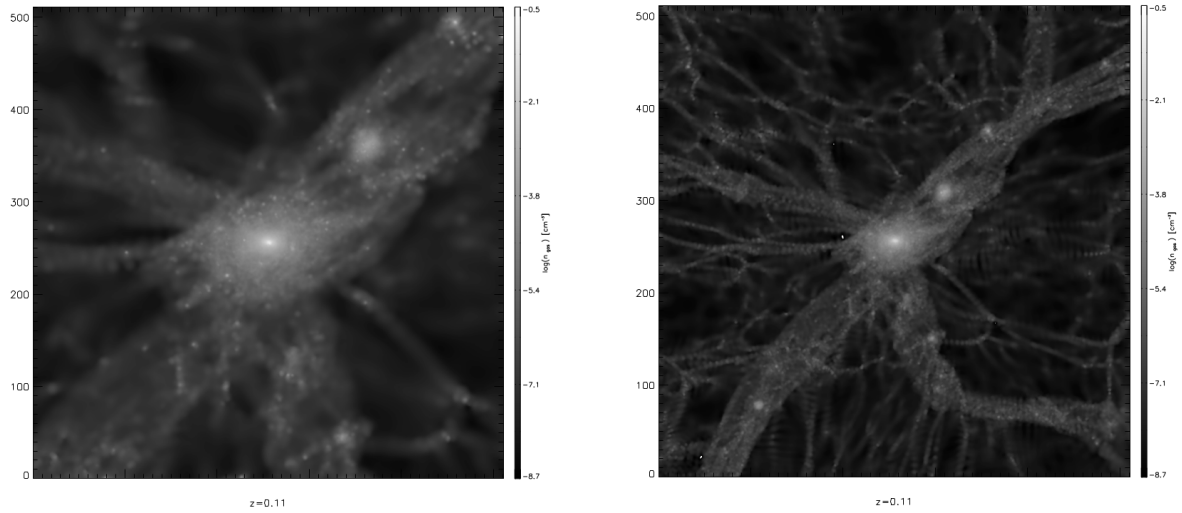

(**a**) (**b**)

Figure 2. Slice cuts at $z = 0.11$ of the LG volume (4^3 Mpc^3, left panel, (**a**)) and the larger 8 cMpc volume (right panel (**b**)) in the GAMESH simulation described in Graziani et al. [25]. The cut intercepts the central MW-like progenitor galaxy and has the same color and grid conventions of Figure 1.

2.1.2. Galaxies with Stars and Metals

To simulate the galaxies forming at the center of each DM halo, we adopted a data-constrained, semi-analytic approach tuned to guarantee that the central halo matches the properties of the Milky Way and that the galaxies in the LG and in the larger 8 cMpc volume respect the scaling relations observed in our Local Volume.

In each galaxy the star-formation rate is computed as proportional to the mass of gas (M_{gas}) and to a certain process efficiency (ϵ_*), chosen to reproduce the observed value of the stellar mass ($M_\star$) in the MW. More specifically, at each given time, stars are formed at a rate SFR $= \epsilon_* M_{gas}/t_{dyn}$, where t_{dyn} is the dynamical time of the hosting halo. In mini-halos (i.e., halos with $T_{vir} < 2 \times 10^4$ K) ϵ_* is

assumed to be $\epsilon_{\rm MH}/\epsilon_* = 2 \times [1 + (T_{\rm vir}/(2 \times 10^4{\rm K}))^{-3}]^{-1}$, as a result of the reduced efficiency of gas cooling. Low-mass stars form according to the critical metallicity scenario [59,60] and assuming a standard, salpeter-like initial mass function (IMF) if the gas metallicity is $Z \geq Z_{cr} = 10^{-4} Z_\odot$; massive Pop III stars form instead if $Z < Z_{cr}$, with a mass $m_{\texttt{Pop III}} = 200\ {\rm M}_\odot$.

Supernova explosions and intermediate mass stars release metals in the gas of the galactic Inter-Stellar Medium (ISM). The model assumes that they instantaneously and homogeneously mix with gas, i.e., we adopt the so called instantaneous recycling approximation (IRA, Tinsley [61]). A fraction of them successively escapes the hosting halos and enriches the diffuse IGM throughout galactic winds. The mass outflow rate of supernova-driven winds is computed as $\dot{M}_{\rm gas,eje} = 2\,\epsilon_{\rm w}\, v_{\rm circ}^{-2}\, \dot{E}_{\rm SN}$, where $\epsilon_{\rm w}$ is the wind efficiency, $v_{\rm circ}$ the host halo circular velocity, and $\dot{E}_{\rm SN}$ is the energy rate released by SN explosions, which depends on the star formation rate and on the stellar IMF (hence, a different value is adopted for Pop III and Pop II stars). The efficiency of winds is also subject to calibration, in order to perform a fine tuning with observed properties.

In summary, the tuning process making GAMESH a data-constrained model involves only two free parameters: the star formation efficiency in Lyα-cooling halos, ϵ_*, and the efficiency of supernova-driven winds, $\epsilon_{\rm w}$. These are calibrated by requiring that the star formation rate, the stellar and gas masses, and the metallicity of the simulated MW galaxy at $z = 0$ match the observed values. Note that some of these quantities are inferred by independent studies and their values can even differ by one order of magnitude, as a result of the alternative tracers adopted to perform the observations or of the modeling strategy used to reconstruct the galaxy components (bulge, disk and halo). The interested reader can find in Kennicutt [62], McKee and Ostriker [63], Kennicutt and Evans [64], Bland-Hawthorn and Gerhard [65] a large collection of critically revised estimates and galaxy modeling techniques. In Graziani et al. [25] we have shown that by adopting $\epsilon_* = 0.09$ and $\epsilon_{\rm w} = 0.0016$ we can easily reproduce the stellar mass and the mass of gas and metals in the MW ISM at $z = 0$.

The accurate feedback implemented in GAMESH has been also proven to reproduce many scaling relations observed in our Local Universe [25,50], as well as a plausible SF history of a MW-like galaxy. In the redshift range $0 < z < 4$ the star formation rate (SFR), stellar, gas, and metal masses of the MW progenitors are in agreement with recent observations [66], although their gas fractions have a shallower evolution in the 3 Gyr period between $z = 2.5$ and $z = 1$. Moreover, the distribution of the most massive MW progenitors is consistent with the fundamental plane of metallicity (FPZ) [67,68] and aligned with the fundamental metallicity relation (FMR) [69].

In Ginolfi et al. [44], after introducing a model of dust production, we compared the chemical properties of dwarf galaxies with the DGS and KINGFISH [70] catalogs showing that the observed sample of low-stellar and low-metallicity galaxies is well covered by our simulation. Additional details on the statistics of star forming objects at $z = 0$ are shown in Appendix A of Marassi et al. [50]: the stellar mass of the GAMESH galaxies largely covers the low-end of the observed sample ($\mathrm{Log}(M_\star/M_\odot) > 6.5$), while the high-mass population of the ALLSMOG sample has a limited coverage due to the bias introduced by the size of our simulated volume. Finally note that the mass metallicity relation at $z = 0$ of the simulated data has a trend in good agreement with the observed relation, as shown in the same appendix.

2.1.3. Radiative Feedback on Star Formation

Depending on the problem at hand, GAMESH can adopt different prescriptions to account for the contribution of radiative feedback. In semi-analytic working mode GAMESH assumes instant reionization, i.e., only galaxies of mass $M_h > M_4(z) = 3 \times 10^8 M_\odot (1+z)^{-3/2}$ ($M_h > M_{30}(z) = 2.89 \times M_4(z)$) can form stars prior to (after) reionization, which is assumed to complete at $z = 6$. In this case the star formation efficiency in mini-halos is decreased $\propto T_{vir}^{-3}$, to mimic the effects of a homogeneous Lyman–Werner background. When GAMESH runs in full feedback mode, it performs a full radiative transfer simulation and the formation of stars is not regulated by the halo mass but by

photo-ionization feedback, i.e., by the temperature of the gas in the IGM. In this way we follow with accuracy the process of reionization of the environments in which MW progenitors and dwarf galaxies evolve in redshift and the model accounts for the inhomogeneities intrinsic in the reionization process and due to the presence of the cosmic web.

Radiative transfer simulations are performed at the redshift z_i of each snapshot and start propagating photons for a duration corresponding to the physical time separating z_i and $z_{(i+1)}$; the resulting 3D maps of the gas ionization fractions ($x_{\mathtt{gas}(z_i)}$) and temperature ($T_{\mathtt{gas}(z_i)}$) are used as initial conditions of the subsequent run at z_{i+1}. Our RT adopts a Monte Carlo-based scheme implementing 3D ray tracing of ionizing radiation and a gas medium composed by H and He, atomic metals and dust. The ionizing packets have N_γ photons per frequency, and they cross the gas distribution derived from the DM grids. At each cell crossing, the total optical depth τ is computed and the amount of absorbed photons evaluated as $N_{abs} = N_\gamma(1 - e^\tau)$. This is further used to calculate the ionization fractions x_s of all the s species and the gas temperature $T_{\mathtt{gas}}$ of the crossed cell. The interested reader can find more technical references in [42,43].

The list of ionizing sources is provided in the box grid by converting the properties of the star forming galaxies (Pop II/Pop III SFR, Z_*) into ionizing sources with specific spectral properties. The ionization rates and spectral shapes of Pop II stars are computed accordingly to Bruzual A. and Charlot [71] and to an assumed IMF in the mass range $[0.1 - 100]M_\odot$. A different spectral shape and ionization rate are then associated with each of the Pop II star forming galaxy, also depending on its population lifetimes t_* and stellar metallicity Z_*. Finally, a grid of pre-computed spectra integrated in specific lifetime bins $t_* \in \{0.001, 0.01, 0.1, 0.4, 1.0, 4.0, 13.0\}$ Gyr and stellar metallicity $Z_* \in \{0.005, 0.2, 0.4, 1.0, 2.5\}Z_\odot$ is used to derive the spectrum and ionization rate. Pop III stars are assumed to have an ionization rate per solar mass, $\dot{N}_\gamma = 1.312 \times 10^{48}$ [photons $\mathrm{s}^{-1}/\mathrm{M}_\odot$] [72] (corresponding to $\mathrm{M}_* \sim 200\ \mathrm{M}_\odot$), averaged on a lifetime of about 2.2 Myr. Their SED is modeled as a black body spectrum at temperature $T_{BB} = 10^5$ K.

Figure 3 shows an example of the irregular temperature pattern created by the progress of reionization in a slice cut of the cosmic volume analyzed in Graziani et al. [24]: photo-ionized bubbles expand from the star forming halos depending on a complex series of radiative transfer effects modulated by the surrounding, irregular, cosmic web; as a consequence they have an inhomogeneous impact on the next generations of star forming galaxies. To make this picture more clear, in the same figure we over-plotted iso-contours of the gas number density distribution (see caption for more details). It should be noted that while the above results are clearly showing a significant impact of the reionization process on small galaxies, a direct extrapolation of them is not possible to the new generation of DM simulations shown in Figure 2a,b, as they differ not only in scale but also in mass and spatial resolution. For the above reasons a new set of GAMESH simulations accounting for detailed reionization is planned (Graziani et al., in prep.).

Feedback on star formation is implemented by evaluating the gas temperature of each galaxy environment, defined as the cell of the grid in which the galaxy spatial coordinates belong to. In this scheme, the gas distribution surrounding halos relies on the spatial resolution of the RT ($\Delta L = L_b/N_c$) and we compare the virial radius R_{vir} of the galactic halo with $\Delta L/2$. If $2R_{vir}/\Delta L \leq 0.1$, the galactic environment is mainly set up in the cell containing its center of mass; its ionization fractions and temperatures are then $x_{\mathtt{gal}} = x_{\mathtt{cell}}$, $T_{\mathtt{gal}} = T_{\mathtt{cell}}$. If, on the other hand, $2R_{vir}/\Delta L > 0.1$ the gas reservoir of the galaxy could extend to the surrounding cells and $T_{\mathtt{gal}}$ is assigned by volume averaging across them. It should be noted that the threshold value 0.1 depends on the grid resolution and it could require additional tuning for higher N_c. Once assigned for each galaxy, $x_{\mathtt{gal}}$ is used to evaluate the mean molecular weight μ of the gas and then to calculate the virial temperature of the galactic halo T_{vir} (see the formulas in Barkana and Loeb [73]). If $T_{\mathtt{gal}} < T_{vir}$, star formation in the galaxy is allowed in the successive step and a new list of star forming galaxies with their SFR, stellar metallicity and population type is provided to the next step.

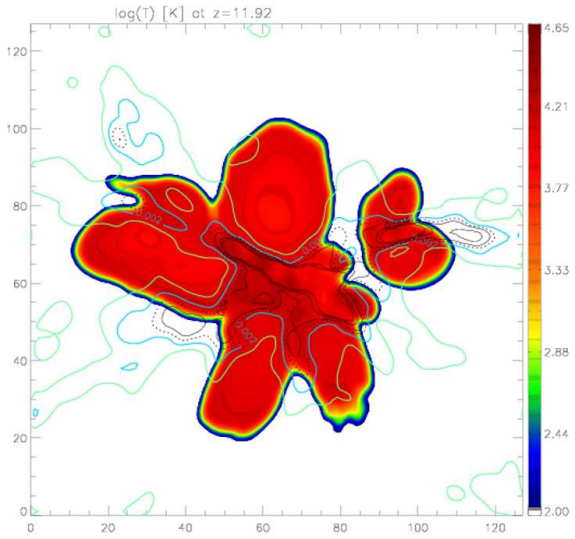

Figure 3. Slice cut at $z \approx 12$ of the logarithm of the gas temperature (Log$T$ [K], from blue ($\approx$100 K) to red ($\approx 5 \times 10^4$ K)) as predicted by the GAMESH simulation described in Graziani et al. [24] and including inhomogeneous reionization simulated by radiative transfer. The box size of this image is 2 cMpc, centered on the MW forming galaxy and it is projected on a Cartesian grid of 128^3 cells. Over-plotted to the temperature map we show some iso-contours of the gas number density $n_{\rm gas}$ corresponding to 10^{-3} cm^{-3} (solid green), 2.0×10^{-3} cm^{-3} (solid cyan), 3.0×10^{-3} cm^{-3} (dashed black), 4.0×10^{-3} cm^{-3} (solid black).

2.2. Stellar Binaries

On top of the galaxy framework described above, the new generation of GAMESH simulations introduces additional constraints to the model of cosmic star formation by accounting for binary systems [46,50]. GAMESH relies on a binary population synthesis (BPS) code, which is capable to follow the stellar and dynamical evolution of a binary system, once its initial conditions are specified. Adhering to the statistical principle that star formation is a stochastic process and that a fraction $f_{2\star}$ regulates how many binaries are formed for each event of a newly generated M$_\star$, GAMESH assigns in each galaxy with SFR > 0 a mass of binaries $M_{2,\star} = f_{2\star} \times$M$_\star$. The properties and evolution of stars in the binary are simulated as a function of the metallicity of the gas ($Z_{\rm gas}$) from which they form, while the dynamical parameters of the system are randomly sampled from pre-assigned dynamical distributions.

The combination of these parameters is used to generate a large database of pre-computed binary systems from which to randomly sample $M_{2,\star}$, as detailed in Section 2.3. Before providing more technical details on the current implementation, it is worth to mention that while our scheme is not necessarily linked to a specific BPS, so far we adopted the code SeBa (http://www.sns.ias.edu/starlab/seba/), in its recently modified version by Mapelli et al. [74].

The algorithm of SeBa was originally developed by Portegies Zwart and Verbunt [8] and Nelemans et al. [75] to follow the evolution of a binary system by accounting for a detailed stellar and dynamical evolution scheme including: stellar composition, winds, mass transfer and accretion, magnetic braking, common envelope phase, supernova kicks, and gravitational radiation. Mapelli et al. [74] successively modified the original code to include the gas metallicity dependence in the evolution of stellar components [76], in winds [49,77], and in the remnant formation [78]. Furthermore, SeBa is an open source code which can be easily adapted and extended to account for more stellar properties (e.g., the stellar and binary spins) and to explore additional physical constraints which could become available in future observations, as discussed in Marassi et al. [50].

In particular, the databases currently adopted by GAMESH contain a large number of binary systems (from 2×10^6 to 2×10^7), spanning different ranges of combination of dynamical initial conditions, randomly selected from independent distribution functions (see Schneider et al. [46],

Marassi et al. [50] for more details). Each database spans $k = 1, ..., 11$ different values of the stellar metallicity, covering the range $0.01 \leq Z/Z_{\odot} \leq 1$. At fixed k, the following initial conditions apply:

- a Kroupa Initial Mass Function (IMF, Kroupa [79]) regulates the distribution of the primary stellar mass, $m_{1,\star}$, in a suitable mass range, while the secondary star has a mass $m_{2,\star}$ generated according to a flat distribution for the mass ratio $q = m_{1,\star}/m_{2,\star}$ with $0.1 < q \leq 1$;
- the initial semi-major axis (a) has a flat distribution in $\log(a)$ (see Portegies Zwart and Verbunt [8]), ranging from $0.1\ R_{\odot}$ (Roche lobe contact) up to $10^6\ R_{\odot}$;
- the eccentricity e of the binary is sampled from a thermal distribution $f(e) = 2e$ in the interval $[0, 1]$ [80].

A list of the currently available databases can be found in Appendix B of Marassi et al. [50], where their usage is also described, based on their statistical significance. Finally, it is important to point out that GAMESH can change its databases by selecting a different BPS, if required by a specific problem. For example, the MOBSE code [13] is a recent alternative to SeBa which offers many improvements in the treatment of metallicity-dependent stellar evolution, new prescriptions for core-collapse supernovae (SNe) and accounts for the dependence of stellar winds on the Eddington factor. Another possibility is provided by the SEVN code [81], which is very promising to explore the binary systems generated in the low-metallicity regime. In Appendices B,C of Marassi et al. [50], more details on the adopted databases and their properties are provided, also depending on the scientific problem at hand.

2.3. Formation and Coalescence Sites

Here we describe how GAMESH uses the BPS databases to associate binaries with star forming galaxies and how compact binary systems evolve along the hierarchical assembly of structures, until their coalescence occurs.

Consider a certain redshift z_i and the list $j \in \{1, ..., N\}$ of star forming halos ($\mathrm{SFR}_{j,i} > 0$) having gas metallicity $Z_{j,i}$. The newly formed stellar mass in binaries is defined, in each halo, as ${M_{2\star}}^{j,i} = f_{2\star} \times {M_{\star}}^{j,i}$ (The binary fraction $f_{2\star}$ is assumed to be redshift independent). To predict which binary belongs to ${M_{2\star}}^{j,i}$, GAMESH first identifies the metallicity bin k by checking that $Z_{k-1} < Z_{j,i} < Z_{k+1}$ and then saturates the value of ${M_{2\star}}^{j,i}$ by randomly sampling binary systems contained in the $k-$bin. It should be noted that if the scientific problem requires to investigate only a specific family of binaries (e.g., compact stars), the above sampling can be simplified by considering the fraction of ${M_{2\star}}^{j,i}$ contained in the IMF mass interval in which compact objects form. For example, Marassi et al. [50] investigated the population of massive binaries generating GW150914-like events by adopting a sampling database in the IMF mass range of $[8.0, 100.0]$ $\mathrm{M}_{\odot}$ and with an assumed SALPETER-like shape; in this way only ~ 14 % of the total mass in binaries ${M_{2\star}}^{j,i}$ required random sampling.

Thanks to the particle-based merger-tree of GAMESH (see Section 2.1.1), galaxies hosting the formation of binaries can be unequivocally identified with their lower redshift descendants, in which coalescence occurs. The cosmic history of each DM halo and the binaries living in its galaxy can also be followed through dynamical events: halo mergers, tidal interactions, and halo disruptions. The baryonic evolution of the associated galaxy can be investigated as well by assuming that its stellar mass (modeled at the center of each DM halos) is transferred from ancestors to descendants by scaling with the DM mass transfer ratio. This assumption also guarantees that there is no ambiguity in the transfer of the associated binary systems along the cosmological evolution from progenitor to descendant galaxies.

By repeating the above algorithm in all the $j-$halos and along the redshift evolution, we can then track all the cosmic history of binary systems, consistently with the star formation history. In summary:

- GAMESH correlates the temporal evolution of binary systems living in galaxies with the large scale process of structure formation, down to $z = 0$.

- Our approach is particularly effective for small dwarf galaxies, because of the many feedback processes accounted for, which strongly impact the evolution of small objects.
- The algorithm described above is sufficiently general to follow both the gravitational and the electromagnetic emission from all the sampled binaries systems, not necessarily the ones evolving into BHBH, BHNS and NSNS compact binaries. Their electromagnetic emission during the stellar evolution phases, in particular, can be additionally modeled with great details thanks to the rich set of information provided by the BPS on stellar radii, surface temperature, evolutionary status, and efficiency of mass transfer exchange. For example, by adopting SeBa, it is possible to track all the stellar stages during the binary evolution: from their proto-stellar phase to their X-rays pulsar or radio pulsar phases, if the components evolve into a neutron stars. This information is also provided as function of time for each system so that the radiative properties of the binary population can be modeled consistently with the galaxy formation process. In this way also the sources accounted for in the radiative scenario are significantly improved.
- As star forming galaxies are populated by the statistical principle of random sampling, the method requires convergence tests. An example of this validation procedure is provided in Marassi et al. [50], Appendixes B and C.

3. Results and Model Predictions

Here we illustrate the kind of predictions the GAMESH model can provide. In Section 3.1 we show the evolution of the halos hosting the birth of binaries originating GW150914-like signals, while Section 3.2 explores the time evolution of the candidate binary systems.

3.1. Evolution of Birth and Coalescence Hosts

Thanks to the particle-based merger tree of GAMESH, once a galaxy is identified as hosting the birth of a stellar binary evolving into a coalescing system, its cosmic assembly can be described in both dark and baryonic matter so that the dynamical origin and metallicity of its stellar component can be theoretically understood.

In Marassi et al. [50] we investigated the early assembly of high redshift dwarf galaxies hosting the birth of stellar binaries originating GW150914-like signals. We have shown that multiple dynamical channels are available for the formation of suitable hosts. For example, dwarfs born at the edge of the cosmic volume can effectively escape the gravitational potential of the central MW and live as isolated low-redshift small galaxies at the time the gravitational signal is generated. More complicated histories exist as well, as star forming low metallicity dwarf galaxies can derive from an assembly history involving many companions, merging together. In Figure 4 we show an unpublished example taken from the cited study; from top to bottom panels contain the redshift evolution of $M_{\rm vir}$, SFR, Z of three halos (indicated by different line colors and symbols) which contribute the assembly of the final dwarf galaxy hosting a candidate for the GW150914 signal. It is evident that after an episode of star formation occurring before the end of reionization (red halo) the halos continue to assemble their gas and metals from the IGM without producing stars; they will finally merge into a single object which experiences its episode of star formation below $z \sim 2.5$ (not shown in the figure). This resulting dwarf, which remained undetectable in the redshift range $2.5 < z < 6.5$ due to its negligible stellar content, silently accumulated its gas mass and a very low metal content; from the above conditions a massive stellar binary can still form at relatively low redshift and evolve in a BHBH system with masses compatible with the generation of GW150914. Note that the coalescing compact binary also requires a coalescing time t_c compatible with the LIGO–VIRGO observed redshift; the orbital parameters suitable to generate the adequate value of t_c will be investigated in the next section.

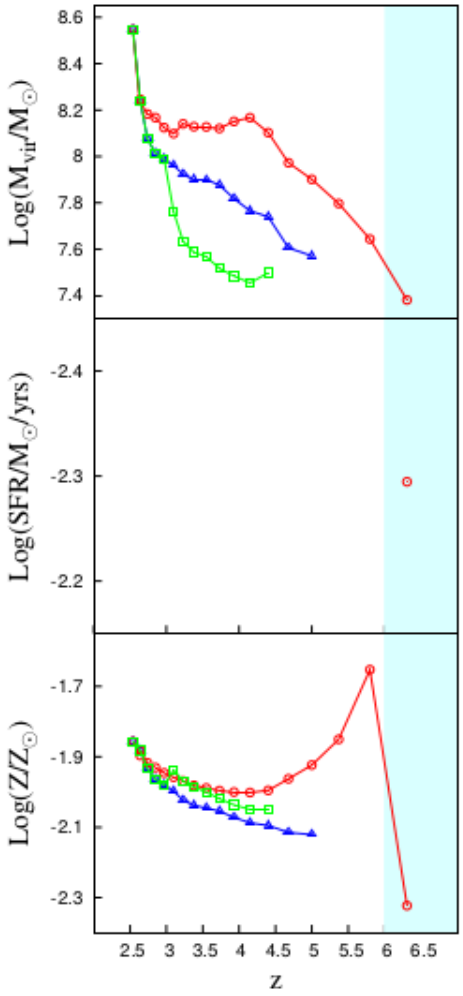

Figure 4. Redshift evolution of $\log(M_{\rm vir}/M_\odot)$ (**top panel**), $\log({\rm SFR}/M_\odot)$ (**middle panel**), and $\log({\rm Z}/Z_\odot)$ (**bottom panel**) of three halos assembling a final one which will host a stellar binary evolving into a BHBH generating GW150914 Marassi et al. [50]. In each panel different evolving halos are indicated by different symbols and colors. The epoch of the assumed reionization is highlighted with a cyan shadow.

Finally note that a similar analysis can be performed on the coalescence sites by simply following the merger tree of the first host, down to the coalescence redshift of each binary. This question is extensively investigated in Schneider et al. [46], Marassi et al. [50].

3.2. Evolution of Stellar Binaries

Once a stellar binary is randomly associated with a star forming halo, the BPS database adopted by GAMESH provides the detailed time evolution of the system from its birth as stellar pair, down to the time of coalescence as compact binary. The values of both stellar progenitor types and their successive BH masses, as well as the orbital parameters of the binary system (i.e., semi-major axis a and eccentricity e), are generally tracked by the BPS each time a change occurs in the stellar evolution of the components. In this section we show the statistics of these quantities targeting on candidate binary systems for GW150914. Their selection is based on the masses of the BH components and the redshift range in which the emission of the GW signal is predicted by the model. In the case of GW150914 we then simultaneously require that $\mathrm{M}_{1,\mathrm{BH}} \sim [32.6\text{–}40.4]\ \mathrm{M}_\odot$, $\mathrm{M}_{2,\mathrm{BH}} \sim [26.2\text{–}33.6]\ \mathrm{M}_\odot$ and the redshift of coalescence z_c is within $z_c \in [0.06, 0.12]$. Once the above requirements are applied to the entire redshift evolution of our galaxies, GAMESH selects 183 unique binary systems from the SeBa database (Note

that these systems can occur more than one time across galaxies and redshifts), all found in the three metallicity bins at $Z \leq 0.05\ Z_{\odot}$.

For each SeBa system we have then access to the evolution of its stars and orbital parameters: semi-major axis (a) and eccentricity (e). In the case of GW150914 we note that the stellar progenitors evolve into BHs on very rapid time scales with respect to the successive black hole merger times: all the above systems form a BHBH binary within $t_{f,c} \in$ [3.52–3.78] Myr, while the successive coalescence time t_c [82] spans several Gyrs and has a wider distribution depending on both the chirp mass of the binary (The chirp mass of a compact binary system is defined as $\mathcal{M} \equiv \mu^{3/5} M^{2/5}$, where μ and M are the reduced and total mass of the binary, respectively) and the values of a and e set up at the time of BHBH formation.

Figure 5a,b show the component masses of stellar progenitors and resulting black holes, all created within $t_{0,\star} \approx 3.6$ Myr for GW150914. The stellar progenitors have stellar masses in Zero Age Main Sequence (ZAMS) phase $M_{\star} > 80\ M_{\odot}$ while it should be noted that the upper limit shown in panel (a) is imposed by the chosen IMF mass range. To prove the existence of more massive stellar candidates we should adopt a different BPS, suitable to describe the stellar formation and evolution at very low gas metallicity. We will explore this problem in a future study by creating a binary database with SEVN [12,81], a new generation BPS targeting the evolution of very massive and low-metallicity binary systems (i.e., masses ranging in the Pop III – Pop II transition regime (i.e., $M_{\star} > 100\ M_{\odot}$)).

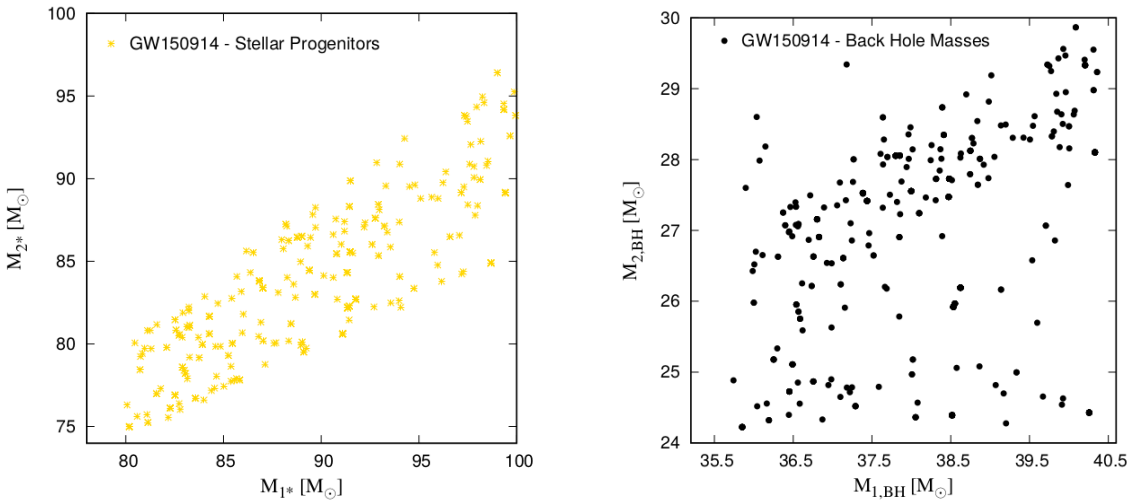

(**a**) (**b**)

Figure 5. Primary and secondary mass of the stellar progenitors (left panel (**a**)) and equivalent masses of their BHs (right panel (**b**)) in the GAMESH simulation described in Marassi et al. [50].

By comparing panel (a) and (b) it is immediately evident that the dynamical evolution of the binary strongly affects the mass of the formed BHs, also breaking the original mass distribution of the two stellar components: for an assigned mass of the primary BH a significant spread in mass of the secondary is in fact allowed in the right panel. We verified that a large number of the SeBa systems shown here are flagged during their evolution as detached systems with a continuous mass-transfer. Note that the formation of a BH is still a subject of intense debate due to the large uncertainties in modeling the collapse process through plasma instabilities (see for e.g., [83]) and that their impact is not accounted for by the SeBa code. More recent BPS models, such as MOBSE [13] and SEVN [12] improved the stellar evolution of the binary components in many of the above aspects and the SeBa predictions for lower BH masses should require additional benchmark with these new models. As described in Section 2.3, the GAMESH binary database has been designed to be BPS-independent so that the predictions made on top of the cosmological evolution can be reinforced by running different BPSs.

Once the compact binary is formed, the redshift of its coalescence (and hence the one of its galaxy host) is set up by t_c. In SeBa t_c is computed as $t_c = t_{0,\mathrm{BH}}(e_{0,\mathrm{BH}}) \times f(e_{0,\mathrm{BH}})$, where:

$$t_{0,\mathrm{BH}} = \frac{c^5}{G^3} \frac{5a_{0,\mathrm{BH}}^4}{256M^2\mu}, \tag{1}$$

$$f(e) = (1 + \frac{73}{24}e^2 + \frac{37}{96}e^4)(1 - e^2)^{-7/2}. \tag{2}$$

and then it primarily depends on both the chirp mass $\mathcal{M}$ and the evolution of a and e within $t_{0,\star}$. In Figure 6a,b we show how the statistical distribution of the above orbital parameters evolves from the birth of the binary (dashed gold histograms) to the time at which the BHBH forms (solid black histograms). In both panels it is clear that these histograms reflect the initial distribution functions chosen to generate the BPS database as described in Section 2.2: systems form in a wide eccentricity range with a moderate prevalence of very eccentric systems $e \approx 1$ and an initial semi-major axis which picks around $a \approx 10^3$ AU. Within $t_{0,\star}$ all the binaries circularize with eccentricity parameter $e_{0,\mathrm{BH}} < 0.23$ and $a_{0,\mathrm{BH}}$ picking at a strongly reduced distance of $a_{0,\mathrm{BH}} \approx 40$ AU. Note, on the other hand, that from Equations (1) and (2) the contribution of the eccentricity to the coalescence time is moderated by the $f(e)$ function while the semi-major axis contributes strongly with a tight $a_{0,\mathrm{BH}}^4$ dependence.

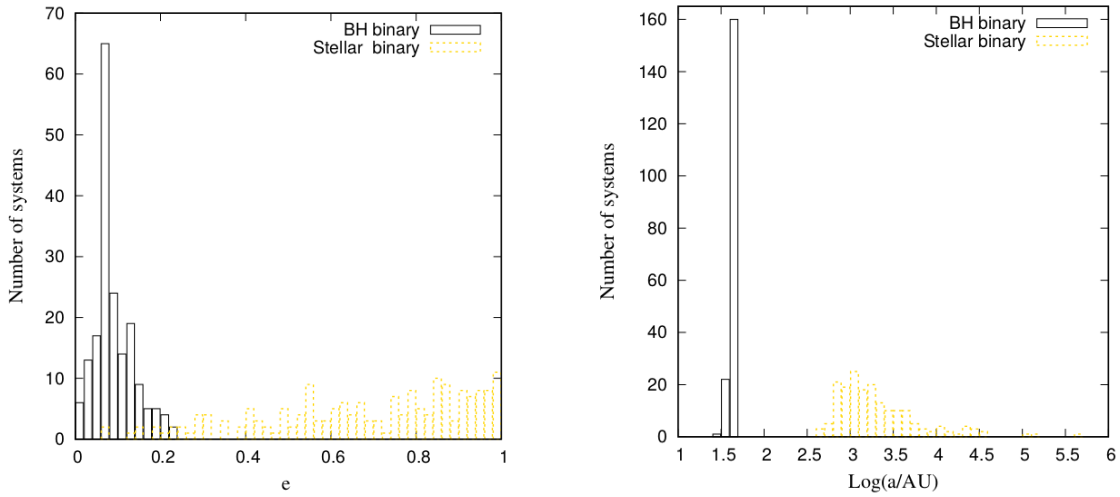

(**a**) (**b**)

Figure 6. Eccentricity (left panel, (**a**)) and semi-major axis (right panel (**b**)) distributions at the times of stellar binary formation (gold-dashed histograms) and at the successive initial times of the BHBH systems (solid-black histograms).

The distribution of t_c as function of $\mathcal{M}$ is shown in Figure 7 for all the GW150914 candidates. The points clearly show an indiscernible dependence of t_c from the chirp mass, while for $\mathcal{M} > 0.0043$, only systems with $t_c > 9$ Gyrs are allowed. Interestingly, and independently on $\mathcal{M}$, the largest sample of points has a cosmologically relevant coalescence time ($t_c > 8$ Gyr) mainly set up by the semi-major axis, also suggesting that the binary progenitors generating GW150914-like events can likely originate from high redshift dwarfs [46,50].

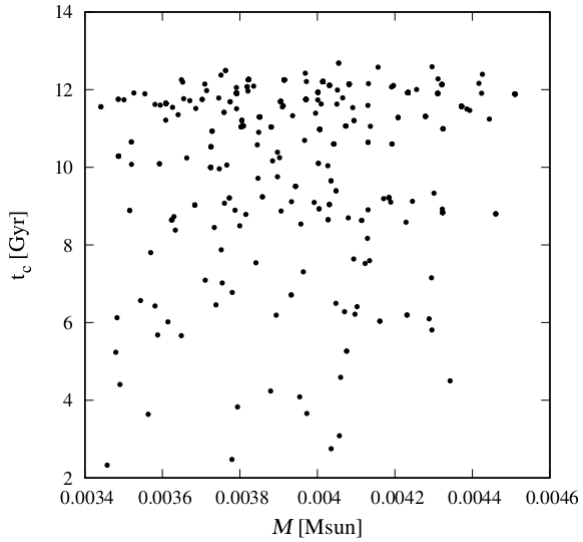

Figure 7. Coalescence time t_c of all the SeBa binaries generating GW150914 as a function of their chirp mass $\mathcal{M}$.

4. Conclusions

In this paper we have described how the galaxy formation model GAMESH was recently extended and improved to consistently account for the evolution of compact binary systems along the cosmological assembly of a MW-like galaxy and its dwarf satellites. We have shown the predictive capability of the GAMESH model in interpreting the evolution of galaxies hosting both the birth and coalescence of compact binaries originating gravitational wave signals like the GW150914 event, detected by the LIGO–VIRGO collaboration.

In particular:

- GAMESH includes a rich set of feedback processes capable to constraint the high redshift evolution of small dwarf galaxies, fragile to mechanical, chemical and radiative feedback;
- thanks to the data-constrained nature of our model, GAMESH is capable to match a large set of properties of the central MW-like galaxy and naturally reproduces the scaling relations observed in the local redshift universe;
- by coupling the galaxy evolution with a large database of binary systems evolving in compact objects, GAMESH predicts the galaxy hosts in which coalescence events occurs;
- by focusing on the binaries generating GW150914-like signals in dwarfs galaxies, we have shown that complex cosmic histories can connect birth and coalescence hosts. While the masses of the BHBH binaries depend on the gas metallicity of the birth dwarfs and the dynamical evolution of the stellar progenitors, the coalescence time t_c selects the coalescence hosts and mainly depends on the initial value of the BHBH semi-major axes.

Future studies will focus on performing detailed reionization simulations to asses the impact of a realistic inhomogeneous process on the evolution of high-redshift dwarfs and on interpreting the large number of events which will become available by integrating the contributions of the O1-O3 LIGO–VIRGO observational runs.

Funding: LG acknowledges support from the Amaldi Research Center funded by the MIUR program "Dipartimento di Eccellenza" (CUP:B81I18001170001).

Acknowledgments: The author is indebted to Stefania Marassi and Raffaella Schneider for continuously supporting the GAMESH model, for enlightening discussions and many aspects of stellar and black hole evolution in binary systems and for a significant help in improving the accuracy of the cited references.

Conflicts of Interest: The author declares no conflict of interest.

References

1. Abbott, B.P.; Abbott, R.; Abbott, T.D.; Abernathy, M.R.; Acernese, F.; Ackley, K.; Adams, C.; Adams, T.; Addesso, P.; Adhikari, R.X.; et al. Binary Black Hole Mergers in the First Advanced LIGO Observing Run. *Phys. Rev. X* **2016**, *6*, 041015. [CrossRef]
2. Abbott, B.P.; Abbott, R.; Abbott, T.D.; Abernathy, M.R.; Acernese, F.; Ackley, K.; Adams, C.; Adams, T.; Addesso, P.; Adhikari, R.X.; et al. Observation of Gravitational Waves from a Binary Black Hole Merger. *Phys. Rev. Lett.* **2016**, *116*, 061102. [CrossRef] [PubMed]
3. Abbott, B.P.; Abbott, R.; Abbott, T.D.; Abernathy, M.R.; Acernese, F.; Ackley, K.; Adams, C.; Adams, T.; Addesso, P.; Adhikari, R.X.; et al. GW151226: Observation of Gravitational Waves from a 22-Solar-Mass Binary Black Hole Coalescence. *Phys. Rev. Lett.* **2016**, *116*, 241103. [CrossRef] [PubMed]
4. Abbott, B.P.; Abbott, R.; Abbott, T.D.; Abernathy, M.R.; Acernese, F.; Ackley, K.; Adams, C.; Adams, T.; Addesso, P.; Adhikari, R.X.; et al. Astrophysical Implications of the Binary Black-hole Merger GW150914. *Astrophys. J. Lett.* **2016**, *818*, L22. [CrossRef]
5. The LIGO Scientific Collaboration; The Virgo Collaboration; Abbott, B.P.; Abbott, R.; Abbott, T.D.; Abraham, S.; Acernese, F.; Ackley, K.; Adams, C.; Adhikari, R.X.; et al. GWTC-1: A Gravitational-Wave Transient Catalog of Compact Binary Mergers Observed by LIGO and Virgo during the First and Second Observing Runs. *arXiv* **2018**, arXiv:1811.12907; reprinted in *Phys. Rev. X* **2019**, *9*, 031040. [CrossRef]
6. KAGRA Collaboration; LIGO Scientific Collaboration; Virgo Collaboration. Prospects for observing and localizing gravitational-wave transients with Advanced LIGO, Advanced Virgo and KAGRA. *Living Rev. Relativ.* **2018**, *21*, 3. [CrossRef]
7. O'Shaughnessy, R.; Bellovary, J.M.; Brooks, A.; Shen, S.; Governato, F.; Christensen, C.R. The effects of host galaxy properties on merging compact binaries detectable by LIGO. *Mon. Not. Roy. Astron. Soc.* **2017**, *464*, 2831–2839. [CrossRef]
8. Portegies Zwart, S.F.; Verbunt, F. Population synthesis of high-mass binaries. *Astron. Astrophys.* **1996**, *309*, 179–196.
9. Dominik, M.; Belczynski, K.; Fryer, C.; Holz, D.E.; Berti, E.; Bulik, T.; Mandel, I.; O'Shaughnessy, R. Double Compact Objects. II. Cosmological Merger Rates. *Astrophys. J.* **2013**, *779*, 72. [CrossRef]
10. Belczynski, K.; Holz, D.E.; Bulik, T.; O'Shaughnessy, R. The first gravitational-wave source from the isolated evolution of two stars in the 40–100 solar mass range. *Nature* **2016**, *534*, 512–515. [CrossRef]
11. Mandel, I.; de Mink, S.E. Merging binary black holes formed through chemically homogeneous evolution in short-period stellar binaries. *Mon. Not. Roy. Astron. Soc.* **2016**, *458*, 2634–2647. [CrossRef]
12. Spera, M.; Mapelli, M. Very massive stars, pair-instability supernovae and intermediate-mass black holes with the sevn code. *Mon. Not. Roy. Astron. Soc.* **2017**, *470*, 4739–4749. [CrossRef]
13. Giacobbo, N.; Mapelli, M.; Spera, M. Merging black hole binaries: The effects of progenitor's metallicity, mass-loss rate and Eddington factor. *Mon. Not. Roy. Astron. Soc.* **2018**, *474*, 2959–2974. [CrossRef]
14. Postnov, K.; Kuranov, A. Black hole spins in coalescing binary black holes. *Mon. Not. Roy. Astron. Soc.* **2019**, *483*, 3288–3306. [CrossRef]
15. Portegies Zwart, S.F.; McMillan, S. Black hole mergers in the universe. *Astrophys. J.* **2000**, *528*, L17. [CrossRef]
16. O'Leary, R.M.; Rasio, F.A.; Fregeau, J.M.; Ivanova, N.; O'Shaughnessy, R.W. Binary mergers and growth of black holes in dense star clusters. *Astrophys. J.* **2006**, *637*, 937–951. [CrossRef]
17. Sadowski, A.; Belczynski, K.; Bulik, T.; Ivanova, N.; Rasio, F.A.; O'Shaughnessy, R.W. The Total Merger Rate of Compact Object Binaries in the Local Universe. *Astrophys. J.* **2008**, *676*, 1162. [CrossRef]
18. Ziosi, B.M.; Mapelli, M.; Branchesi, M.; Tormen, G. Dynamics of stellar black holes in young star clusters with different metallicities—II. Black hole–black hole binaries. *Mon. Not. Roy. Astron. Soc.* **2014**, *441*, 3703–3717. [CrossRef]
19. Mapelli, M. Massive black hole binaries from runaway collisions: The impact of metallicity. *Mon. Not. Roy. Astron. Soc.* **2016**, *459*, 3432–3446. [CrossRef]
20. Antonini, F.; Rasio, F.A. Merging black hole binaries in galactic nuclei: Implications for advanced-LIGO detections. *Astrophys. J.* **2016**, *831*, 187. [CrossRef]
21. Carr, B.; Kuhnel, F.; Sandstad, M. Primordial Black Holes as Dark Matter. *Phys. Rev.* **2016**, *D94*, 083504. [CrossRef]

22. Somerville, R.S.; Popping, G.; Trager, S.C. Star formation in semi-analytic galaxy formation models with multiphase gas. *Mon. Not. Roy. Astron. Soc.* **2015**, *453*, 4337–4367. [CrossRef]
23. Henriques, B.M.B.; White, S.D.M.; Thomas, P.A.; Angulo, R.; Guo, Q.; Lemson, G.; Springel, V.; Overzier, R. Galaxy formation in the Planck cosmology—I. Matching the observed evolution of star formation rates, colours and stellar masses. *Mon. Not. Roy. Astron. Soc.* **2015**, *451*, 2663–2680. [CrossRef]
24. Graziani, L.; Salvadori, S.; Schneider, R.; Kawata, D.; de Bennassuti, M.; Maselli, A. Galaxy formation with radiative and chemical feedback. *Mon. Not. Roy. Astron. Soc.* **2015**, *449*, 3137–3148. [CrossRef]
25. Graziani, L.; de Bennassuti, M.; Schneider, R.; Kawata, D.; Salvadori, S. The history of the dark and luminous side of Milky Way-like progenitors. *Mon. Not. Roy. Astron. Soc.* **2017**, *469*, 1101–1116. [CrossRef]
26. Abbott, B.P.; Abbott, R.; Abbott, T.D.; Abernathy, M.R.; Acernese, F.; Ackley, K.; Adams, C.; Adams, T.; Addesso, P.; Adhikari, R.X.; et al. Localization and broadband follow-up of the gravitational-wave transient GW150914. *Astrophys. J.* **2016**, *826*, L13. [CrossRef]
27. Perna, R.; Lazzati, D.; Farr, W. Limits on Electromagnetic Counterparts of Gravitational-wave-detected Binary Black Hole Mergers. *Astrophys. J.* **2019**, *875*, 49. [CrossRef]
28. Brocato, E.; Branchesi, M.; Cappellaro, E.; Covino, S.; Grado, A.; Greco, G.; Limatola, L.; Stratta, G.; Yang, S.; Campana, S.; et al. GRAWITA: VLT Survey Telescope observations of the gravitational wave sources GW150914 and GW151226. *Mon. Not. Roy. Astron. Soc.* **2018**, *474*, 411–426. [CrossRef]
29. Stratta, G.; Ciolfi, R.; Amati, L.; Bozzo, E.; Ghirlanda, G.; Maiorano, E.; Nicastro, L.; Rossi, A.; Vinciguerra, S.; Frontera, F.; et al. THESEUS: A key space mission concept for Multi-Messenger Astrophysics. *Adv. Space Res.* **2018**, *62*, 662–682. [CrossRef]
30. Abbott, B.P.; Abbott, R.; Abbott, T.D.; Abraham, S.; Acernese, F.; Ackley, K.; Adams, C.; Adhikari, R.X.; Adya, V.; Affeldt, C.; et al. Binary Black Hole Population Properties Inferred from the First and Second Observing Runs of Advanced LIGO and Advanced Virgo. *arXiv* **2018**, arXiv:1811.12940.
31. Mapelli, M.; Giacobbo, N.; Ripamonti, E.; Spera, M. The cosmic merger rate of stellar black hole binaries from the Illustris simulation. *Mon. Not. Roy. Astron. Soc.* **2017**, *472*, 2422–2435. [CrossRef]
32. Vogelsberger, M.; Genel, S.; Springel, V.; Torrey, P.; Sijacki, D.; Xu, D.; Snyder, G.; Nelson, D.; Hernquist, L. Introducing the Illustris Project: Simulating the coevolution of dark and visible matter in the Universe. *Mon. Not. Roy. Astron. Soc.* **2014**, *444*, 1518–1547. [CrossRef]
33. Artale, M.C.; Mapelli, M.; Giacobbo, N.; Sabha, N.B.; Spera, M.; Santoliquido, F.; Bressan, A. Host galaxies of merging compact objects: Mass, star formation rate, metallicity and colours. *Mon. Not. Roy. Astron. Soc.* **2019**. [CrossRef]
34. Lamberts, A.; Garrison-Kimmel, S.; Hopkins, P.F.; Quataert, E.; Bullock, J.S.; Faucher-Giguère, C.A.; Wetzel, A.; Kereš, D.; Drango, K.; Sanderson, R.E. Predicting the binary black hole population of the Milky Way with cosmological simulations. *Mon. Not. Roy. Astron. Soc.* **2018**, *480*, 2704–2718. [CrossRef]
35. Hopkins, P.F.; Kereš, D.; Oñorbe, J.; Faucher-Giguère, C.A.; Quataert, E.; Murray, N.; Bullock, J.S. Galaxies on FIRE (Feedback In Realistic Environments): Stellar feedback explains cosmologically inefficient star formation. *Mon. Not. Roy. Astron. Soc.* **2014**, *445*, 581–603. [CrossRef]
36. Wetzel, A.R.; Hopkins, P.F.; Kim, J.h.; Faucher-Giguère, C.A.; Kereš, D.; Quataert, E. Reconciling Dwarf Galaxies with ΛCDM Cosmology: Simulating a Realistic Population of Satellites around a Milky Way-mass Galaxy. *Astrophys. J. Lett.* **2016**, *827*, L23. [CrossRef]
37. Schaye, J.; Crain, R.A.; Bower, R.G.; Furlong, M.; Schaller, M.; Theuns, T.; Dalla Vecchia, C.; Frenk, C.S.; McCarthy, I.G.; Helly, J.C.; et al. The EAGLE project: Simulating the evolution and assembly of galaxies and their environments. *Mon. Not. Roy. Astron. Soc.* **2015**, *446*, 521–554. [CrossRef]
38. Pillepich, A.; Springel, V.; Nelson, D.; Genel, S.; Naiman, J.; Pakmor, R.; Hernquist, L.; Torrey, P.; Vogelsberger, M.; Weinberger, R.; et al. Simulating galaxy formation with the IllustrisTNG model. *Mon. Not. Roy. Astron. Soc.* **2018**, *473*, 4077–4106. [CrossRef]
39. Norman, M.L.; Chen, P.; Wise, J.H.; Xu, H. Fully Coupled Simulation of Cosmic Reionization. III. Stochastic Early Reionization by the Smallest Galaxies. *Astrophys. J.* **2018**, *867*, 27. [CrossRef]
40. Rosdahl, J.; Katz, H.; Blaizot, J.; Kimm, T.; Michel-Dansac, L.; Garel, T.; Haehnelt, M.; Ocvirk, P.; Teyssier, R. The SPHINX cosmological simulations of the first billion years: The impact of binary stars on reionization. *Mon. Not. Roy. Astron. Soc.* **2018**, *479*, 994–1016. [CrossRef]
41. Schneider, R.; Ferrara, A.; Salvaterra, R.; Omukai, K.; Bromm, V. Low-mass relics of early star formation. *Nature* **2003**, *422*, 869–871. [CrossRef] [PubMed]

42. Graziani, L.; Maselli, A.; Ciardi, B. CRASH3: Cosmological radiative transfer through metals. *Mon. Not. Roy. Astron. Soc.* **2013**, *431*, 722–740. [CrossRef]
43. Graziani, L.; Ciardi, B.; Glatzle, M. X-ray ionization of the intergalactic medium by quasars. *Mon. Not. Roy. Astron. Soc.* **2018**, *479*, 4320–4335. [CrossRef]
44. Ginolfi, M.; Graziani, L.; Schneider, R.; Marassi, S.; Valiante, R.; Dell'Agli, F.; Ventura, P.; Hunt, L.K. Where does galactic dust come from? *Mon. Not. Roy. Astron. Soc.* **2018**, *473*, 4538–4543. [CrossRef]
45. Glatzle, M.; Ciardi, B.; Graziani, L. Radiative transfer of ionizing radiation through gas and dust: The stellar source case. *Mon. Not. Roy. Astron. Soc.* **2019**, *482*, 321–336. [CrossRef]
46. Schneider, R.; Graziani, L.; Marassi, S.; Spera, M.; Mapelli, M.; Alparone, M.; de Bennassuti, M. The formation and coalescence sites of the first gravitational wave events. *Mon. Not. Roy. Astron. Soc.* **2017**, *471*, L105–L109. [CrossRef]
47. Lamberts, A.; Garrison-Kimmel, S.; Clausen, D.R.; Hopkins, P.F. When and where did GW150914 form? *Mon. Not. Roy. Astron. Soc.* **2016**, *463*, L31–L35. [CrossRef]
48. Elbert, O.D.; Bullock, J.S.; Kaplinghat, M. Counting black holes: The cosmic stellar remnant population and implications for LIGO. *Mon. Not. Roy. Astron. Soc.* **2018**, *473*, 1186–1194. [CrossRef]
49. Belczynski, K.; Bulik, T.; Fryer, C.L.; Ruiter, A.; Valsecchi, F.; Vink, J.S.; Hurley, J.R. On the Maximum Mass of Stellar Black Holes. *Astrophys. J.* **2010**, *714*, 1217–1226. [CrossRef]
50. Marassi, S.; Graziani, L.; Ginolfi, M.; Schneider, R.; Mapelli, M.; Spera, M.; Alparone, M. Evolution of dwarf galaxies hosting GW150914-like events. *Mon. Not. Roy. Astron. Soc.* **2019**, *484*, 3219–3232. [CrossRef]
51. Cicone, C.; Bothwell, M.; Wagg, J.; Møller, P.; De Breuck, C.; Zhang, Z.; Martín, S.; Maiolino, R.; Severgnini, P.; Aravena, M.; et al. The final data release of ALLSMOG: A survey of CO in typical local low-M_* star-forming galaxies. *Astron. Astrophys.* **2017**, *604*, A53. [CrossRef]
52. Rémy-Ruyer, A.; Madden, S.C.; Galliano, F.; Lebouteiller, V.; Baes, M.; Bendo, G.J.; Boselli, A.; Ciesla, L.; Cormier, D.; Cooray, A.; et al. Linking dust emission to fundamental properties in galaxies: The low-metallicity picture. *Astron. Astrophys.* **2015**, *582*, A121. [CrossRef]
53. Kawata, D.; Gibson, B.K. GCD+: A new chemodynamical approach to modelling supernovae and chemical enrichment in elliptical galaxies. *Mon. Not. Roy. Astron. Soc.* **2003**, *340*, 908–922. [CrossRef]
54. Kawata, D.; Okamoto, T.; Gibson, B.K.; Barnes, D.J.; Cen, R. Calibrating an updated smoothed particle hydrodynamics scheme within gcd+. *Mon. Not. Roy. Astron. Soc.* **2013**, *428*, 1968–1979. [CrossRef]
55. Hahn, O.; Abel, T. Multi-scale initial conditions for cosmological simulations. *Mon. Not. Roy. Astron. Soc.* **2011**, *415*, 2101–2121. [CrossRef]
56. Planck Collaboration; Ade, P.A.R.; Aghanim, N.; Armitage-Caplan, C.; Arnaud, M.; Ashdown, M.; Atrio-Barandela, F.; Aumont, J.; Baccigalupi, C.; Banday, A.J.; et al. Planck 2013 results. XVI. Cosmological parameters. *Astron. Astrophys.* **2014**, *571*, A16. [CrossRef]
57. Guo, Q.; White, S.; Li, C.; Boylan-Kolchin, M. How do galaxies populate dark matter haloes? *Mon. Not. Roy. Astron. Soc.* **2010**, *404*, 1111–1120. [CrossRef]
58. Ibata, R.; Martin, N.F.; Irwin, M.; Chapman, S.; Ferguson, A.M.N.; Lewis, G.F.; McConnachie, A.W. The Haunted Halos of Andromeda and Triangulum: A Panorama of Galaxy Formation in Action. *Astrophys. J.* **2007**, *671*, 1591–1623. [CrossRef]
59. Schneider, R.; Ferrara, A.; Natarajan, P.; Omukai, K. First Stars, Very Massive Black Holes, and Metals. *Astrophys. J.* **2002**, *571*, 30–39. [CrossRef]
60. Schneider, R.; Omukai, K.; Inoue, A.K.; Ferrara, A. Fragmentation of star-forming clouds enriched with the first dust. *Mon. Not. Roy. Astron. Soc.* **2006**, *369*, 1437–1444. [CrossRef]
61. Tinsley, B.M. Evolution of the Stars and Gas in Galaxies. *Fundam. Cosm. Phys.* **1980**, *5*, 287–388. [CrossRef]
62. Kennicutt, R.C., Jr. Star Formation in Galaxies Along the Hubble Sequence. *Annu. Rev. Astron. Astrophys.* **1998**, *36*, 189–232. [CrossRef]
63. McKee, C.F.; Ostriker, E.C. Theory of Star Formation. *Annu. Rev. Astron. Astrophys.* **2007**, *45*, 565–687. [CrossRef]
64. Kennicutt, R.C.; Evans, N.J. Star Formation in the Milky Way and Nearby Galaxies. *Annu. Rev. Astron. Astrophys.* **2012**, *50*, 531–608. [CrossRef]
65. Bland-Hawthorn, J.; Gerhard, O. The Galaxy in Context: Structural, Kinematic, and Integrated Properties. *Annu. Rev. Astron. Astrophys.* **2016**, *54*, 529–596. [CrossRef]

66. Papovich, C.; Labbé, I.; Quadri, R.; Tilvi, V.; Behroozi, P.; Bell, E.F.; Glazebrook, K.; Spitler, L.; Straatman, C.M.S.; Tran, K.V.; et al. ZFOURGE/CANDELS: On the Evolution of M* Galaxy Progenitors from z = 3 to 0.5. *Astrophys. J.* **2015**, *803*, 26. [CrossRef]
67. Hunt, L.; Magrini, L.; Galli, D.; Schneider, R.; Bianchi, S.; Maiolino, R.; Romano, D.; Tosi, M.; Valiante, R. Scaling relations of metallicity, stellar mass and star formation rate in metal-poor starbursts—I. A Fundamental Plane. *Mon. Not. Roy. Astron. Soc.* **2012**, *427*, 906. [CrossRef]
68. Hunt, L.; Dayal, P.; Magrini, L.; Ferrara, A. Coevolution of metallicity and star formation in galaxies to z$\simeq$ 3.7—I. A Fundamental Plane. *Mon. Not. Roy. Astron. Soc.* **2016**, *463*, 2002. [CrossRef]
69. Mannucci, F.; Cresci, G.; Maiolino, R.; Marconi, A.; Gnerucci, A. A fundamental relation between mass, star formation rate and metallicity in local and high-redshift galaxies. *Mon. Not. Roy. Astron. Soc.* **2010**, *408*, 2115. [CrossRef]
70. Kennicutt, R.C.; Calzetti, D.; Aniano, G.; Appleton, P.; Armus, L.; Beirão, P.; Bolatto, A.D.; Brandl, B.; Crocker, A.; Croxall, K.; et al. KINGFISH—Key Insights on Nearby Galaxies: A Far-Infrared Survey with Herschel: Survey Description and Image Atlas. *Publ. Astron. Soc. Pac.* **2011**, *123*, 1347. [CrossRef]
71. Bruzual A., G.; Charlot, S. Spectral evolution of stellar populations using isochrone synthesis. *Astrophys. J.* **1993**, *405*, 538–553. [CrossRef]
72. Schaerer, D. On the properties of massive Population III stars and metal-free stellar populations. *Astron. Astrophys.* **2002**, *382*, 28–42. [CrossRef]
73. Barkana, R.; Loeb, A. In the beginning: The first sources of light and the reionization of the universe. *Phys. Rep.* **2001**, *349*, 125–238. [CrossRef]
74. Mapelli, M.; Zampieri, L.; Ripamonti, E.; Bressan, A. Dynamics of stellar black holes in young star clusters with different metallicities - I. Implications for X-ray binaries. *Mon. Not. Roy. Astron. Soc.* **2013**, *429*, 2298–2314. [CrossRef]
75. Nelemans, G.; Yungelson, L.R.; Portegies Zwart, S.F. The gravitational wave signal from the Galactic disk population of binaries containing two compact objects. *Astron. Astrophys.* **2001**, *375*, 890–898. [CrossRef]
76. Hurley, J.R.; Tout, C.A.; Pols, O.R. Evolution of binary stars and the effect of tides on binary populations. *Mon. Not. Roy. Astron. Soc.* **2002**, *329*, 897–928. [CrossRef]
77. Vink, J.S.; de Koter, A.; Lamers, H.J.G.L.M. Mass-loss predictions for O and B stars as a function of metallicity. *Astron. Astrophys.* **2001**, *369*, 574–588. [CrossRef]
78. Mapelli, M.; Colpi, M.; Zampieri, L. Low metallicity and ultra-luminous X-ray sources in the Cartwheel galaxy. *Mon. Not. Roy. Astron. Soc.* **2009**, *395*, L71–L75. [CrossRef]
79. Kroupa, P. On the variation of the initial mass function. *Mon. Not. Roy. Astron. Soc.* **2001**, *322*, 231–246. [CrossRef]
80. Heggie, D.C. Binary evolution in stellar dynamics. *Mon. Not. Roy. Astron. Soc.* **1975**, *173*, 729–787. [CrossRef]
81. Spera, M.; Mapelli, M.; Giacobbo, N.; Trani, A.A.; Bressan, A.; Costa, G. Merging black hole binaries with the SEVN code. *Mon. Not. Roy. Astron. Soc.* **2019**, *485*, 889–907. [CrossRef]
82. Postnov, K.A.; Yungelson, L.R. The Evolution of Compact Binary Star Systems. *Living Rev. Relativ.* **2014**, *17*, 3. [CrossRef] [PubMed]
83. Woosley, S.E. Pulsational Pair-instability Supernovae. *Astrophys. J.* **2017**, *836*, 244. [CrossRef]